Overtopping of harbour breakwaters: a comparison of semi-empirical equations, neural networks, and physical model tests

ÁNGELES M. RODRÍGUEZ GIL

JOSÉ F. SÁNCHEZ GONZÁLEZ

RAMÓN GUTIÉRREZ SERRET

VICENTE NEGRO VALDECANTOS

ABSTRACT
This paper reports extensive tests of empirical equations developed by different authors for harbour breakwater overtopping. First, the existing equations are compiled and evaluated as tools for estimating the overtopping rates on sloping and vertical breakwaters. These equations are then tested using the data obtained in a number of laboratory studies performed in the Centre for Harbours and Coastal Studies of the CEDEX, Spain. It was found that the recommended application ranges of the empirical equations typically deviate from those revealed in the experimental tests. In addition, a neural network model developed within the European CLASH Project is tested. The wind effects on overtopping are also assessed using a reduced scale physical model.

Keywords: Experimental facilities; laboratory studies; model effects; overtopping; scale effects; wave-structure interactions; wind

1 Introduction

The ways of assessing overtopping processes range from traditional (semi-empirical or empirical equations and physical model tests) to less conventional (direct measurements of breakwaters, artificial neural networks, and numerical models). In this Note, we asses three of these approaches: semi-empirical equations, physical model tests, and neural networks. The main focus of the paper is on the identification of the application criteria for each of these approaches. First, empirical overtopping equations are compared with a number of physical model tests performed in the CEDEX, Spain. Likewise, the neural network theory based calculation method developed in the European CLASH Project (De Rouck, Van de Walle, & Geeraerts, 2005) is also tested. Second, the wind effects on overtopping are evaluated using tests performed with and without wind in the physical model of the Levante Breakwater.

2 Background

Overtopping is defined as the process of water surpassing the crest of a breakwater and reaching the sheltered area. This phenomenon needs to be accounted for in setting the breakwater's crest level, depending on the volume of water admissible at the rear and the sheltered area's functional and structural factors.

Quantifying overtopping in situ is always problematic due to difficulties in the installation and start up of measuring equipment. Only few measurements have been made on prototypes so far. On the other hand, determining overtopping in reduced scale physical model tests is simple although the obtained data may be affected by the scale effects and thus can only be considered as an approximation of what actually happens at the prototype scale. Nevertheless, physical models are considered to be very useful for estimating potential damage that may occur in the area sheltered by the breakwater. Scale effects in overtopping tests are due to the impossibility of scaling water properties (e.g., the size of drops and spray is similar in the model and at the prototype scale). This is one of the reasons why the overtopping phenomenon is among the processes that are most difficult to reproduce in physical models. Therefore, for a greater approximation of reality, tests in large-size installations generating both waves and wind must be performed. Another issue of the model-prototype interrelation relates to the three-dimensional nature of the phenomenon, especially when the wave incidence on the breakwater is oblique. In such cases, the combination of the running wave formed along the breakwater with the incident wave causes overtopping to concentrate in certain areas with the consequent risks at the rear of the breakwater. To reproduce and account for this effect, overtopping must be studied using three-dimensional tests in large-scale models allowing generation of both waves and wind.

To quantify a breakwater performance, the mean overtopping rate q is usually used and it is defined as the averaged flow rate per unit breakwater width, i.e.

$$q = \frac{1}{t_0}\sum_{i=1}^{N_0} V_i \tag{1}$$

Table 1 Overtopping models: sloping breakwaters

Authors	Structure features	Overtopping model	Dimensionless overtopping rate, Q	Dimensionless freeboard, R
Owen (1980, 1982)	Smooth, impermeable, straight, bermed sloping breakwater	$Q = a\exp(-bR)$	$\frac{q}{gH_sT_{0m}}$	$\frac{R_c}{H_s}\left(\frac{s_{0m}}{2\pi}\right)^{1/2}\frac{1}{\gamma_r\gamma_b\gamma_h\gamma_\beta}$
Goda (1985)*	Vertical and sloping breakwaters		$\frac{q}{\left[2g(H_0')^3\right]^{1/2}}$	$\frac{R_c}{H_0'}$
Bradbury et al. (1988)	Sloping breakwater, rock slope, impermeable and crowned with crown wall	$Q = aR^{-b}$	$\frac{q}{gH_sT_{0m}}$	$\left(\frac{R_c}{H_s}\right)^2\left(\frac{s_{0m}}{2\pi}\right)^{1/2}$
Aminti & Franco (1988)	Sloping breakwater with armour layer formed by a double layer of rocks, cubes or tetrapods on impermeable slope with crown wall	$Q = aR^{-b}$	$\frac{q}{gH_sT_{0m}}$	$\left(\frac{R_c}{H_s}\right)^2\left(\frac{s_{0m}}{2\pi}\right)^{1/2}$
Ahrens & Heimbaugh (1988)	Seven different designs of breakwaters and revetments	$Q = a\exp(-bR)$	$\frac{q}{\left[g(H_s^3)\right]^{1/2}}$	$\frac{R_c}{(H_sL_{0p})^{1/3}}$
Pedersen (1992)	Sloping breakwater, slightly impermeable rubble mound armour layer with crown wall	$Q = R$	$\frac{qT_{0m}}{L_{0m}^2}$	$\frac{H_s}{R_c}$
de Waal & van der Meer (1992)	Sloping breakwater with smooth slope, impermeable and bermed	$Q = a\exp(-bR)$	$\frac{q}{\left[g(H_s^3)\right]^{1/2}}$	$\frac{3.1(R_{u2\%}-R_c)}{H_s}$
van der Meer & Janssen (1995)	Sloping breakwater with smooth slope, impermeable and bermed	$Q = a\exp(-bR)$	$\frac{qs_{0p}^{1/2}}{(g(H_s^3)\tan\alpha)^{1/2}}$ for $\varepsilon_{op} < 2$ $\frac{q}{\left[g(H_s^3)\right]^{1/2}}$ for $\varepsilon_{op} < 2$	$\frac{R_c}{H_s}\frac{s_{0p}^{1/2}}{\tan\alpha}\frac{1}{\gamma_r\gamma_b\gamma_h\gamma_\beta}$ for $\varepsilon_{op} < 2$ $\frac{R_c}{H_s}\frac{1}{\gamma_r\gamma_b\gamma_h\gamma_\beta}$ for $\varepsilon_{op} < 2$
Pedersen (1996)	Sloping breakwater, slightly impermeable, rubble mound armour layer, with crown wall	$Q = R$	$\frac{qT_{0m}}{L_{0m}^2}$	$3.2\times10^{-5}\frac{H_s^5\tan\alpha}{R_c^3A_cB}$
Berenguer & Baonza (2006)	Sloping breakwaters, block or rubble mound armour layer, with crown wall	$Q = \exp(aR-b)$	$\frac{q}{gT_pH_s}$	$\frac{R_{u2\%}^{0.95}A_c^{0.05}}{R_c^{0.7}B^{0.3}}$
Pullen et al. (2007)**	Sloping breakwater without crown wall	$Q = a\exp(-bR)$	$\frac{q}{\left[g(H_{m0}^3)\right]^{1/2}}$	$\frac{R_c}{H_{m0}\gamma_f\,\gamma_\beta}$

*Given as a series of diagrams. **Pullen et al. (2007) provides the overtopping rate by two approaches, probabilistic and deterministic, with empirical coefficients a and b depending on the approach

where t_0 is the observation time, N_0 is the number of waves with heights H_i and periods T_i that reach the structure and produce an overtopping volume V_i per unit crest width. The dimension of the mean overtopping rate q is $m^3\ s^{-1}$ per metre.

Numerous empirical expressions obtained from laboratory tests have been proposed for calculating the overtopping rates. In these expressions, the overtopping rates depend not only on the environmental conditions but also on the model characteristics. Therefore, the empirical relations are only applicable for the ranges of parameters for which they have been obtained. The most typical equations are $Q = a\exp(-bR)$ and $Q = aR^{-b}$, where Q is a dimensionless overtopping rate, R is a dimensionless freeboard (i.e., the height of the breakwater crest above the mean water level), a and b are empirical constants, which are different in the exponential and power-type equations. In addition to the purely empirical relations, the neural NN-OVERTOPPING2 network developed in the EU CLASH Project can also be used for evaluation of q. The EU CLASH Project (De Rouck, Van de Walle, & Geeraerts, 2005) arose from the need to have a generic procedure for estimating the overtopping rates avoiding the use of specific equations which, as stated earlier, are restricted to the conditions for which they have been obtained.

The wind effects on the overtopping processes represent an additional important factor that has not yet been studied in-depth. Only a few physical model tests have been performed where overtopping has been quantified at simultaneously acting wind and waves. The wind typically increases overtopping and the engineers often use this effect to explain observed discrepancies between physical models and prototypes. Using physical model tests where waves were generated with and without wind, Ward, Zhang, Wibner, & Cinotto (1996) determined that the wind effects are due to wave deformation and breaking, wave-structure interaction, increase in water level on the structure, and the contribution of spray to overtopping.

Several authors have compared run-up and overtopping parameters measured at prototypes with those recorded in laboratory tests and with those obtained using the existing empirical equations. Grüne (1982) and Kingston & Murphy (1996) have found that estimates from the empirical equations and physical models were lower than those actually measured. These differences between models and prototypes have motivated the European MAST III Opticrest project (De Rouck, Boone, & Van de Walle, 2001). A key outcome of this project was a finding that the scale effects in physical models typically lead to overtopping values that are approximately 20% lower compared with those measured in prototypes. This discrepancy led to the initiation of the EU CLASH project (De Rouck, Van de Walle, & Geeraerts, 2005) that developed a correction coefficient for the overtopping rate measured in a physical model. This coefficient also accounts for the wind presence. However, the proposed approach is not valid for sloping structures with a crown wall or a parapet protruding from the armour layer.

Tables 1 and 2 compile the equations proposed for calculating the overtopping rates. The equations for sloping breakwaters are shown first (Table 1) followed by the equations for vertical breakwaters (Table 2).

The main variables in Table 1 are: q is the mean overtopping rate per unit structure width, a and b are empirical coefficients specific of each formula, R_c is the crest freeboard of a structure, A_c is the armour crest freeboard, B is the width of structure crest, α is the angle between overall structure slope and the horizontal, H_s is the significant wave height and H_{m0} is the significant wave height from spectral analysis. The subscript 0 refers to deep water condition in the following variables: H_0' is significant wave height, T_{0m} is the average wave period, T_{0p} is the

Table 2 Overtopping models: vertical breakwaters

Authors	Overtopping model	Dimensionless overtopping rate, Q	Dimensionless freeboard, R
Goda (1985)*		$\dfrac{q}{\left[2g(H_0')^3\right]^{1/2}}$	$\dfrac{R_c}{H_0'}$
Franco et al. (1994)	$Q = a\exp(-bR)$	$\dfrac{q}{\left[g(H_s^3)\right]^{1/2}}$	$\dfrac{R_c}{H_s}\dfrac{1}{\gamma_r\gamma_b\gamma_h\gamma_\beta}$
Allsop et al. (1995)	Not impulsive $h_* > 0.3$ $Q = a\exp(-bR)$	$\dfrac{q}{\left[g(H_s^3)\right]^{1/2}}$	$\dfrac{R_c}{H_s}$
	Impulsive $h_* \leq 0.3$ $Q = aR^{-b}$		$h_*\dfrac{R_c}{H_s}$
Pullen et al. (2007)**	Not impulsive ($h_* > 0.3$): $Q = a\exp(-bR)$	$\dfrac{q}{\left[g(H_{m0}^3)\right]^{1/2}}$	$\dfrac{R_c}{H_{m0}}$
	Impulsive ($h_* \leq 0.2$) and broken waves: $Q = aR^{-b}$	$\dfrac{q}{h_*^2\left[g(H_{m0}^3)\right]^{1/2}}$	Impulsive $h_*\dfrac{R_c}{H_{m0}}$
			Broken waves $h_*\dfrac{R_c}{H_s}$

*Given as a series of diagrams. **Pullen et al. (2007) provides the overtopping rate by two approaches, probabilistic and deterministic, with empirical coefficients a and b depending on the approach.

peak wave period, L_{0m} is the mean wave length, L_{0p} is the peak wave length, s_{0m} is the wave steepness at L_{0m}, which is based on T_{0m}, s_{0p} is the wave steepness calculated with L_{0p}, which is based on T_{0p}, $R_{u2\%}$ is the run-up level exceeded by 2% of incident waves, ε_{op} is the surf similarity parameter, also denoted as the Iribarren number, based on s_{0p}. Finally, there are several correction factors to take into account the presence of a berm (γ_b), permeability and roughness (γ_r), flow depth (γ_h) and the possibility of oblique wave attack (γ_β).

In Table 2: h_* is a discriminating parameter, defined as $h_* = 1.35(h_s/H_{m0})(2\pi h_s/gT^2_{m-1,0})$, where h_s is water depth at the toe of a structure and $T_{m\ -\ 1,0}$ is the average wave period defined by m_{-1}/m_0.

3 Physical model tests

The tests presented in this paper were completed in the Maritime Experimentation Laboratory of the CEDEX (Spanish Ministry

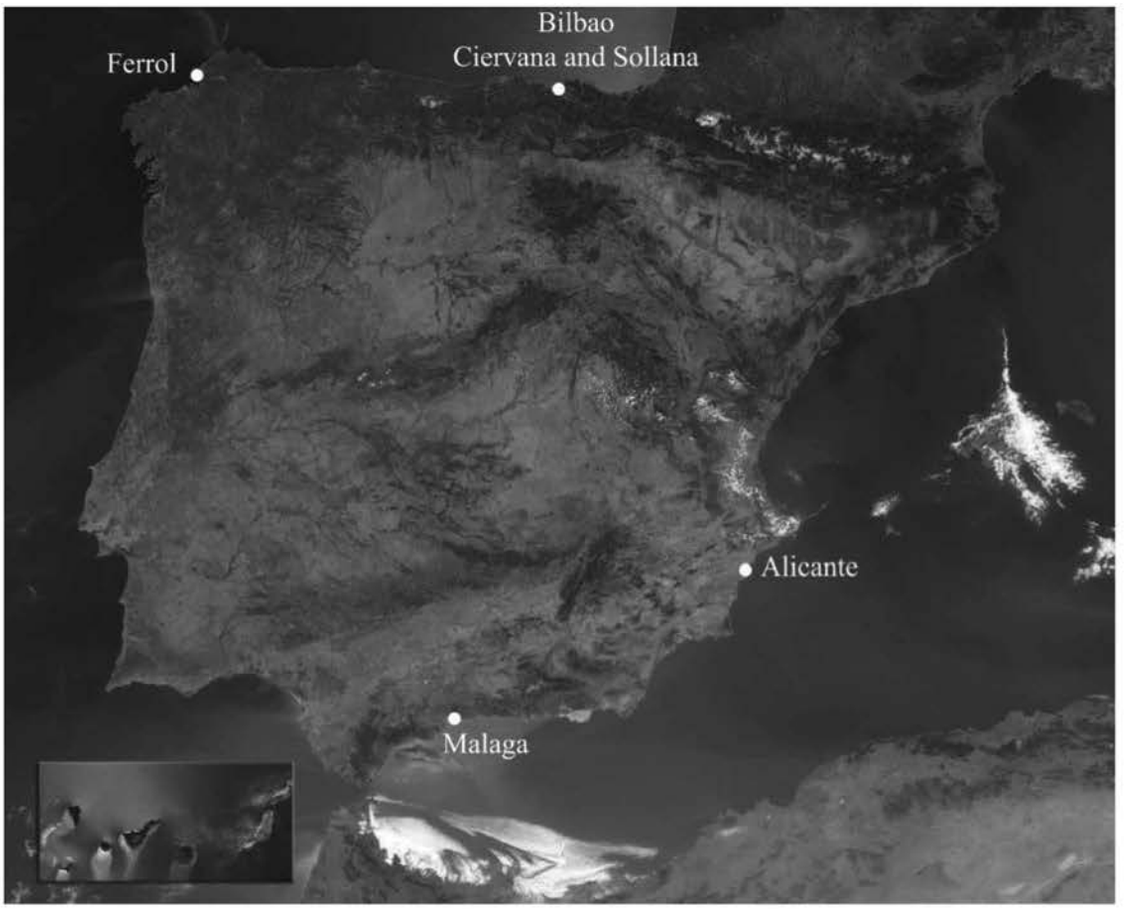

Figure 1 Locations of the breakwaters tested in the laboratory

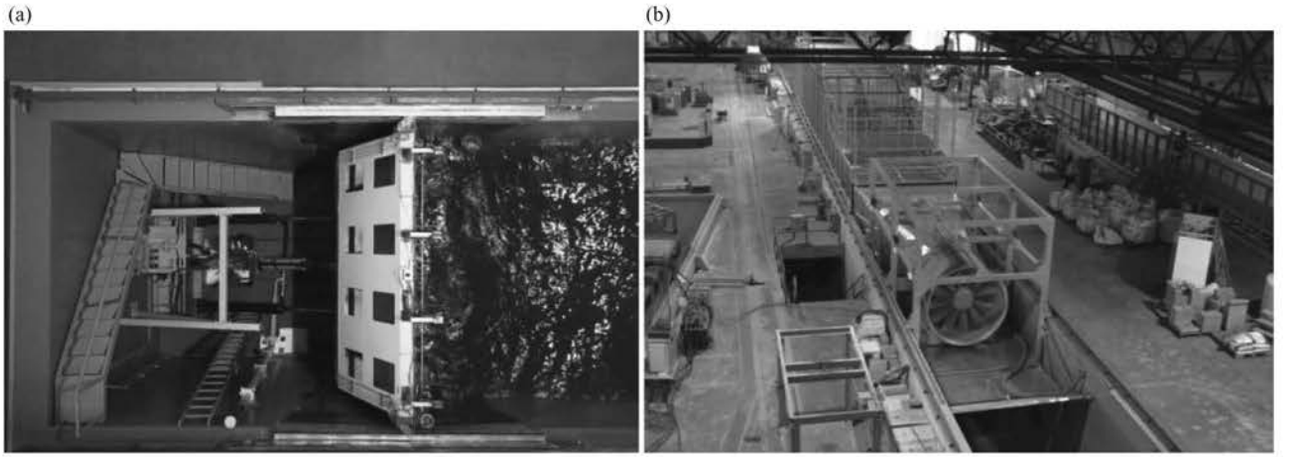

Figure 2 Large Scale Wind and Wave Channel. (a) View of the wave generating paddle and (b) the wind-generating facility

Table 3 Parameters of the tested sloping breakwaters

Breakwater	Crest freeboard of the structure, R_c (m)	Armour crest freeboard of the structure, A_c (m)	Slope of the berm	Crest width of the structure (m)	Main armour layer blocks (t)
Ciervana	18	13.5	1/2	7.5	85
Alicante*	7.5	5.91	A:2/3 B:1/2	4.7	A:20 B:15
Ferrol	18	13	1/1.75	3	90
Sollana	15	12	2/3	10	75

*Two options were tested, A and B.

Table 4 Parameters of the tested vertical breakwater

Breakwater	Crest freeboard of the structure, R_c (m)	Water depth at toe of the structure, h_s (m)	Water depth above berm of the structure, d (m)
Levante	10	31	18.4

Table 5 Characteristics of the tests and the test storm

Breakwater	Waves		Water level (m)	Model Scale
	H_s (m)	T_p (s)		
Ciervana*	5.5–12	19	4.5	1/60
Alicante	4.0–6.0	9, 12	0.5	A:1/40.6 B:1/37
Ferrol	6.4–8.7	14, 18	5	1/43
Sollana	5.4–8.2	11, 13, 15,17	2.5	1/15
Levante**	3.0–7.0	9, 11	0.8	1/20

*Tests were performed with head-on waves and 20° oblique incidence.
**Tests were performed with and without wind.

of Public Works and Transport). The physical models of the breakwaters at Ciervana, Alicante and Ferrol (Fig. 1) were tested in a 46.5 m long, 6.5 m wide and 1.5 m deep wave flume, equipped with a wave generator. Its paddles are hydraulically driven and are able to generate irregular waves with parameters required for the tests. It also has an active reflection absorption system.

The Sollana and Levante physical model tests were carried out in the 90 m long, 3.60 m wide Large Scale Wind and Wave Channel, with depth ranging between 6 m in the wave generation area and 4.50 m in the test area (Fig. 2). The measurements of the following parameters were completed for the different significant wave heights tested: (1) number of overtoppings (counted visually), and (2) volume of water overtopping the crown wall. A water recipient was placed in the central rear area of the crown wall into which the overtopping water poured through a chute supported on the crest. The overtopping recipient hanged from a load cell such that each discharge of water was measured at the moment of pouring into the recipient. The measurements corresponded to a 15 m breakwater length in Sollana and 20 m breakwater length in Levante in

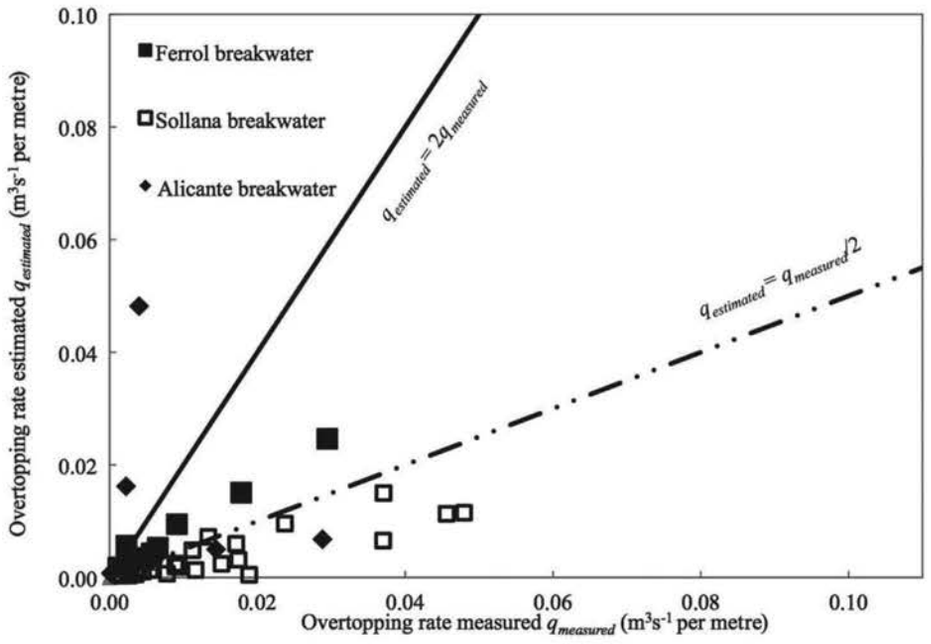

Figure 3 Tests for the Ferrol, Sollana and Alicante breakwaters: comparison with the Bradbury et al. (1988) formula

prototype, which may be considered sufficiently representative breakwater lengths.

Overtopping in the area of the Levante breakwater occurs during south-east storms, thus being enhanced by the wind blowing in the same direction making the mass of water and air move, after running up over the breakwater's crown wall, to its rear. Therefore, these tests were carried out involving wind generation in the CEDEX Large Scale Wind and Wave Channel. Additionally, the overtopping recipient in the Levante tests was subdivided into five compartments to determine the overtopping distribution across the structure. Tables 3 and 4 provide the characteristics of the breakwaters tested.

Various storm waves were generated with spectral characteristics that matched a theoretical predefined Jonswap's spectrum type. Table 5 includes the characteristics of the tests and the storm generated.

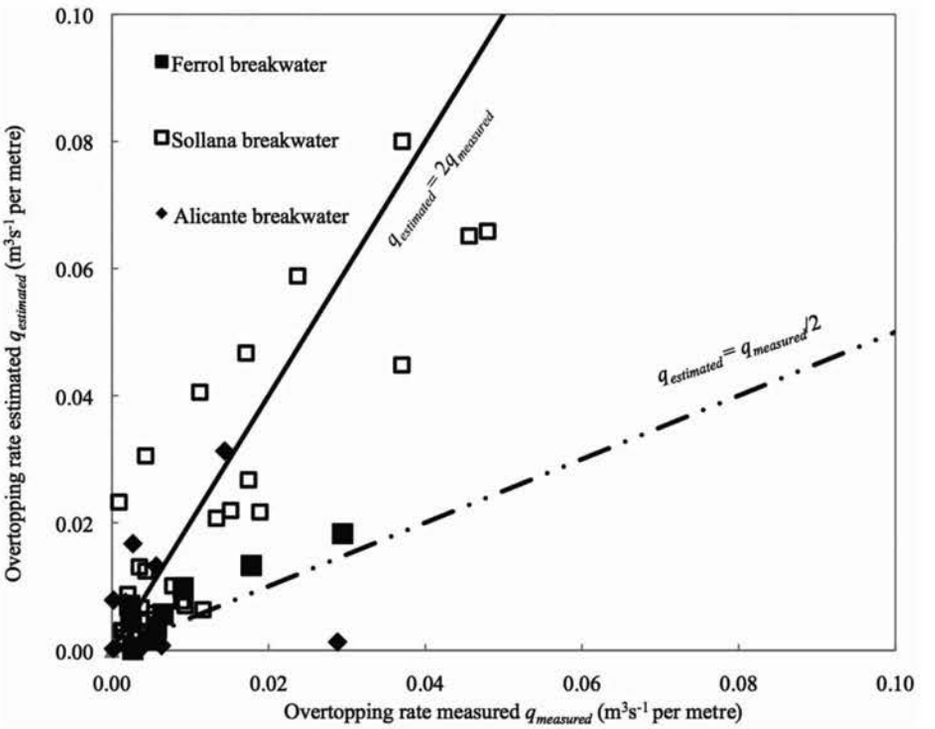

Figure 4 Tests for the Ferrol, Sollana and Alicante breakwaters: comparison with the Aminti et al. (1988) formula

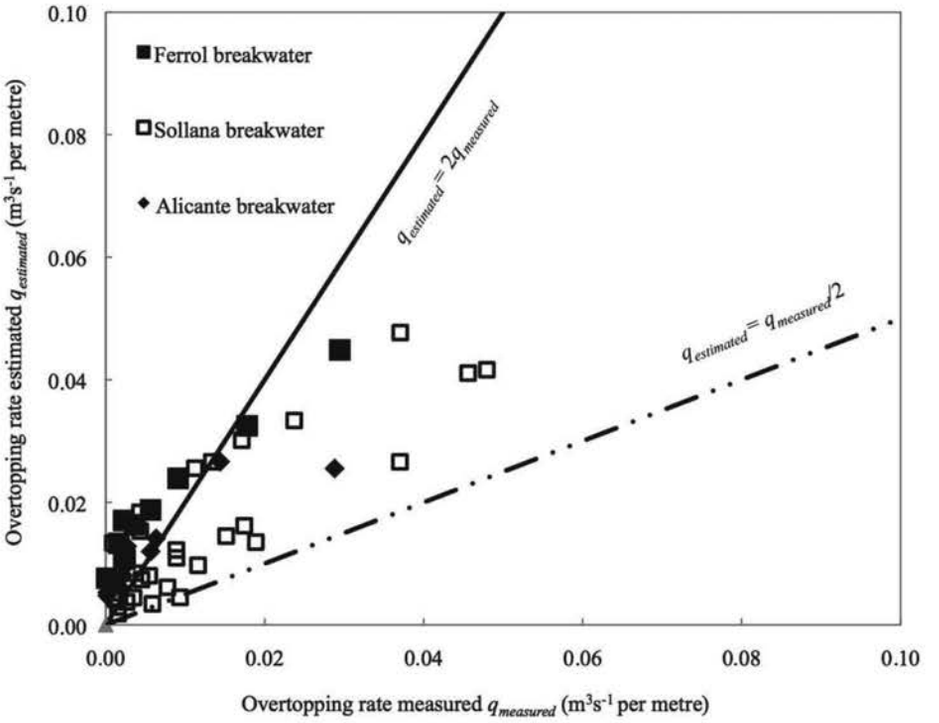

Figure 5 Tests for the Ferrol, Sollana and Alicante breakwaters: comparison with the Pedersen (1992, 1996) formula

4 Comparative analysis: equations, neural networks and physical models

4.1 *Sloping breakwaters: windless tests*

As Figs 3 to 10 show, at lower overtopping rates recorded in the tests (less than 0.02 m^3 s^{-1} per metre) all methods produce high dispersion of the data points, and values up to six times different from those measured in the physical models are predicted. On the other hand, as the measured overtopping rate increases, the predictive equations and neural network match the tests more closely. The best results for overtopping rates higher than 0.05 m^3 s^{-1} per metre are obtained when applying the neural network and Berenguer & Baonza (2006) and Pedersen (1992, 1996) equations. Overall, Figs 3 to 10 lead to the following conclusions.

The best performance of the Bradbury, Allsop, & Stephens (1988) formula is noted for the tests of the Ciervana and

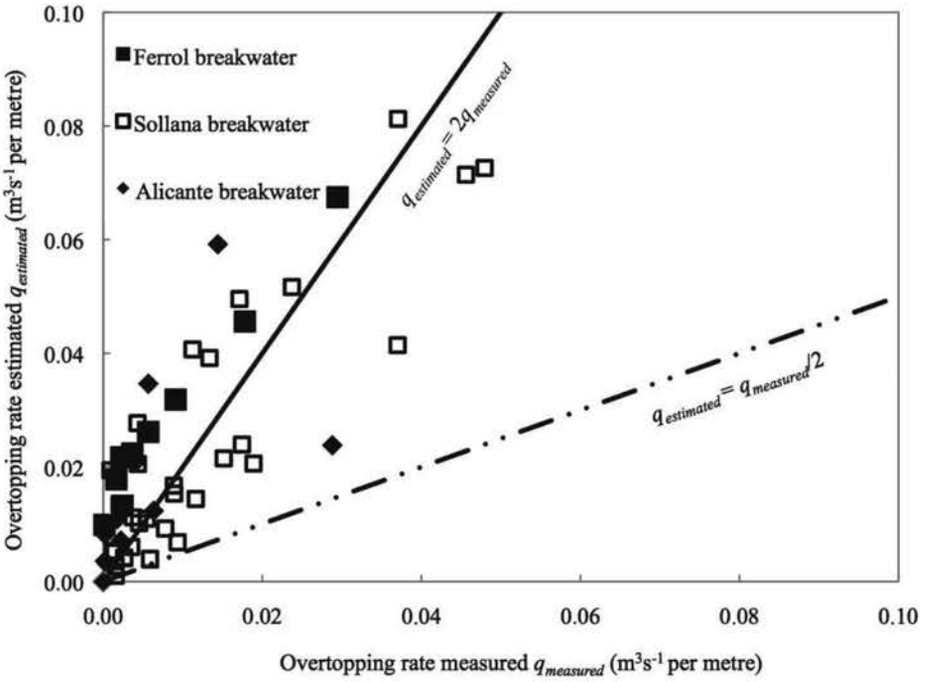

Figure 6 Tests for the Ferrol, Sollana and Alicante breakwaters: comparison with the Berenguer & Baonza (2006) formula

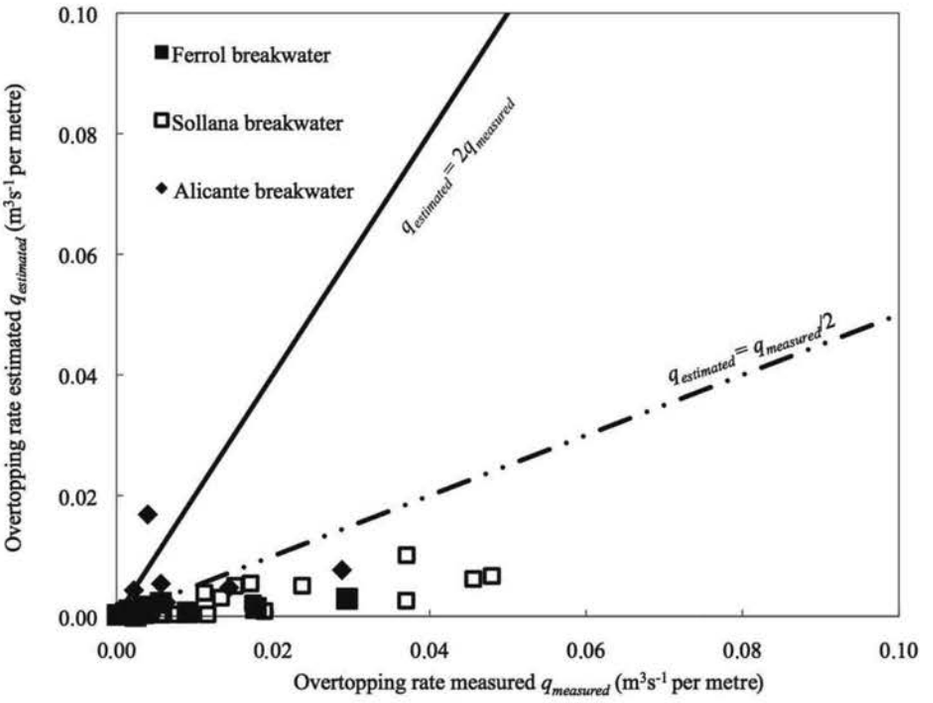

Figure 7 Tests for the Ferrol, Sollana and Alicante breakwaters: comparison with the Pullen et al. (2007) formula (probabilistic approach)

Alicante breakwaters. Most of the conditions required by this equation are fulfilled in both cases. However, the best match in the case of the Ciervana breakwater is obtained in the test with oblique wave incidence, although the equation was obtained for the perpendicular incidence. This inconsistency means that the reliability of the predictions cannot be guaranteed. In the case of the Port of Alicante test, the best match was obtained for both options (A and B) with $T_p = 9$ s, and it may therefore be inferred that the peak period influences the overtopping rate obtained with this method. However, the same tendency is not observed in the Sollana breakwater test. The match is better for $T_p = 17$ s compared with other periods, irrespective of the tide level. For the rest of peak periods tested, approximately the same match is obtained regardless of the peak period and the tide level. Considering next the Aminti & Franco (1988) equation, one should note that its applicability range, highlighted by the authors, is not satisfied in any of the cases analysed. The deviation from the measured data reaches 100% and thus the predictive reliability of the Aminti & Franco (1988) equation is low. Although most conditions of applicability of the

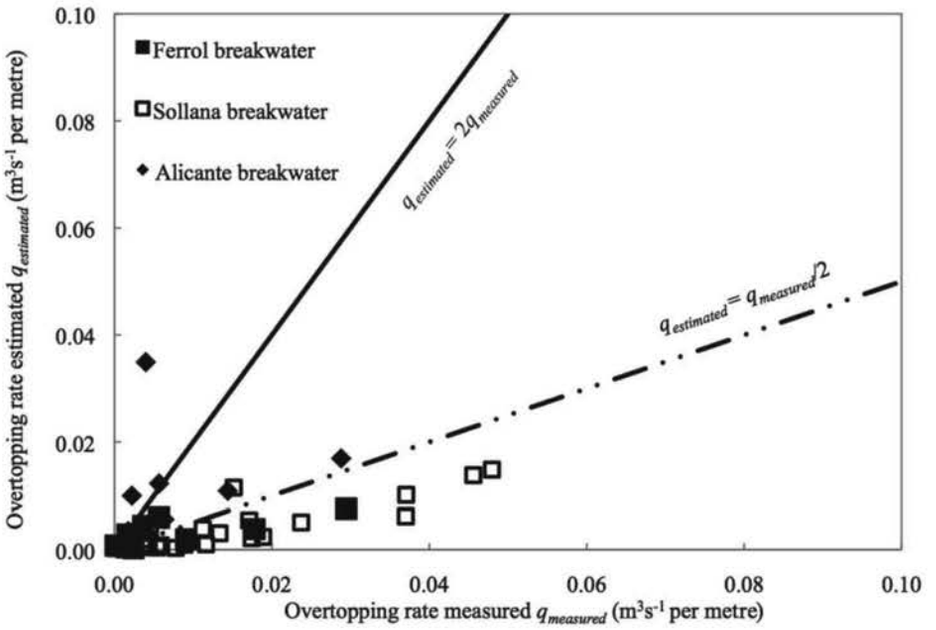

Figure 8 Tests for the Ferrol, Sollana and Alicante breakwaters: comparison with the Pullen et al. (2007) formula (deterministic approach)

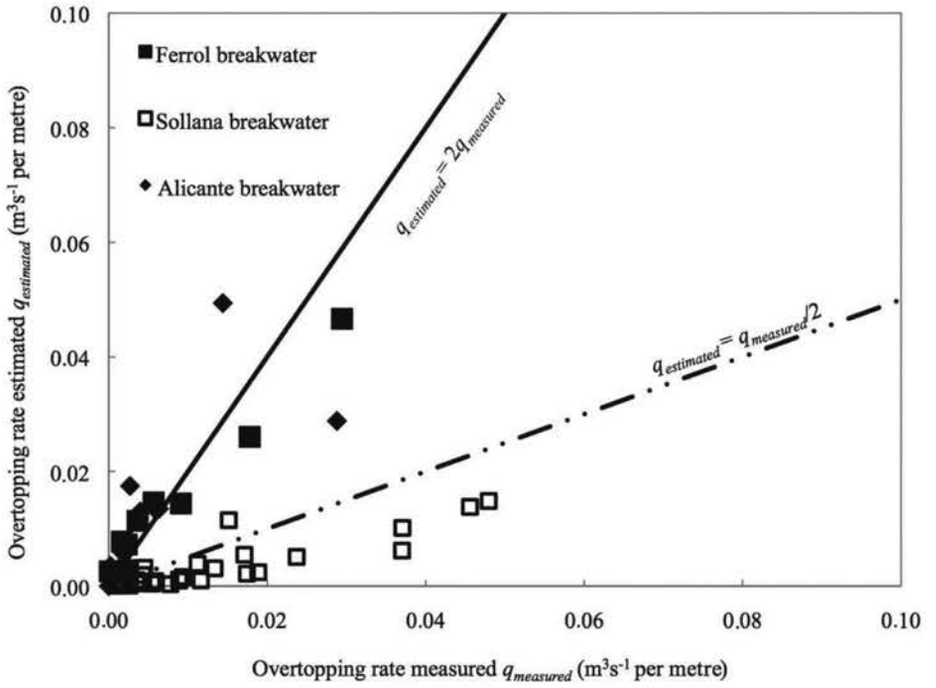

Figure 9 Tests for the Ferrol, Sollana and Alicante breakwaters: comparison with the De Rouck et al. (2005) neural network predictions

Pedersen et al. (1992, 1996) equation are met in our tests, there is one significant deviation. The main armour layer elements in our tests were blocks when the Pedersen (1992, 1996) equation has been proposed for the rubble mound, leading to estimated values being appreciably higher than measured. The Berenguer & Baonza (2006) equation performed better, probably reflecting the fact that the declared applicability conditions for their equation have been closely matched in our tests. The test of the

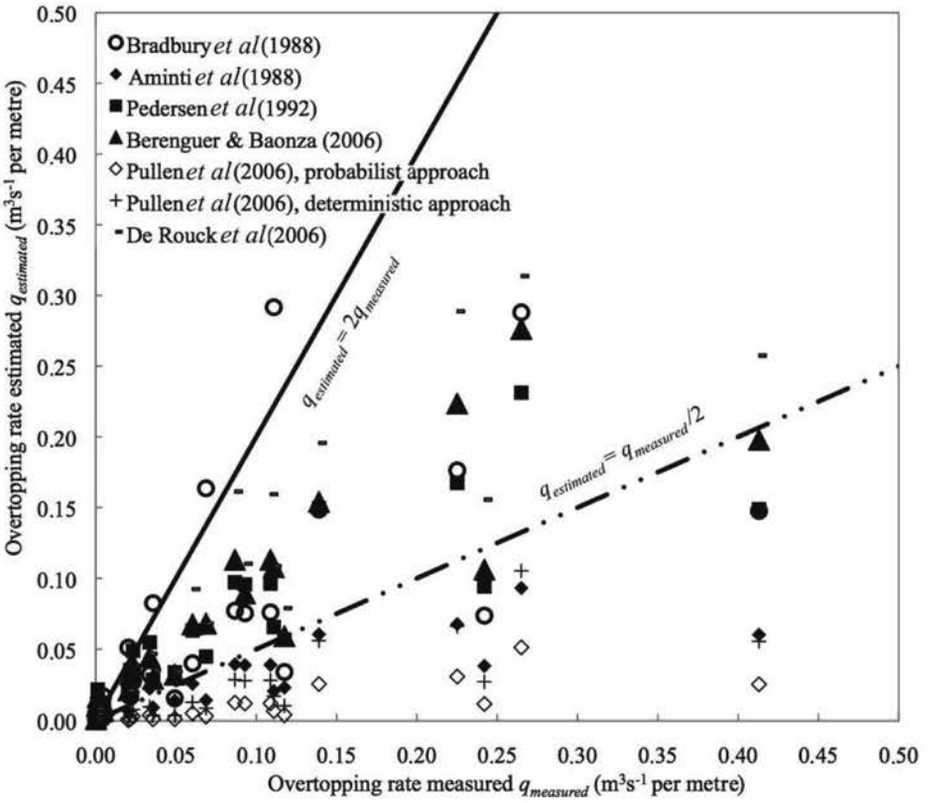

Figure 10 Tests for the Ciervana breakwaters: comparison with the formulas and neural network predictions

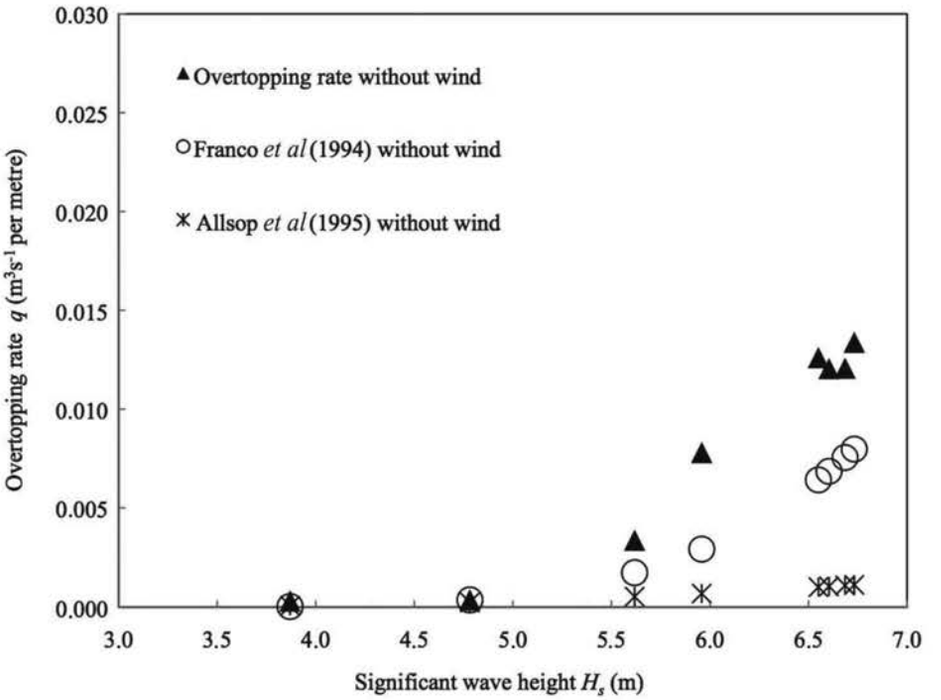

Figure 11 Comparison of the measured overtopping rates with estimates based on the Allsop et al. (1995) and Franco et al. (1994) formulas at $T_p =$ 9 s and no wind

Pullen et al. (2007) equation (known as EurOtop) was not as successful and there is a tendency for the predicted values to be biased low. The neural network model NN-OVERTOPPING2 of De Rouck et al. (2005) tends to give values between one and two times the overtopping rate measured. The worst match was obtained for the Port of Alicante breakwater tests where the overtopping rate estimate appeared to be much higher than the measured value. Note that the results obtained for the Ciervana breakwater are shown separately in Fig. 10 due to a different scale of the overtopping rates in this test.

4.2 *Vertical breakwater: wind effects*

Figures 11 and 12 show the total overtopping rates (i.e., the sums of compartmented values) for the two tested periods T_p, i.e., 9 and 11 s. The results obtained in the tests are compared with predictions based on the Allsop, Besley, & Madurini (1995) and Franco, de Gerloni, & van der Meer (1994) formulas. The overtopping rates were greater in the tests with wind and waves compared with the case when wind was absent (Figs 13 and 14).

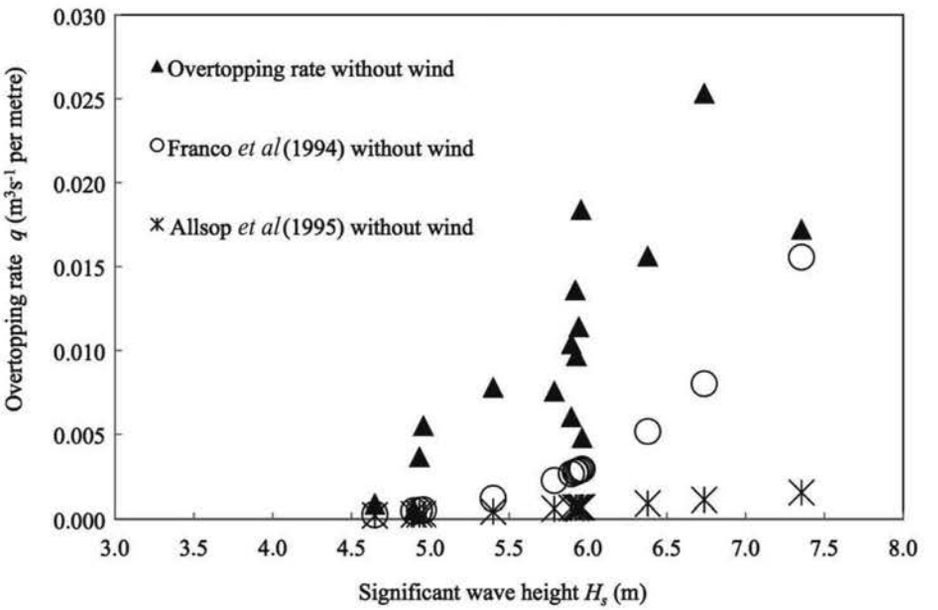

Figure 12 Comparison of the measured overtopping rates with estimates based on the Allsop et al. (1995) and Franco et al. (1994) formulas at $T_p =$ 11 s and no wind

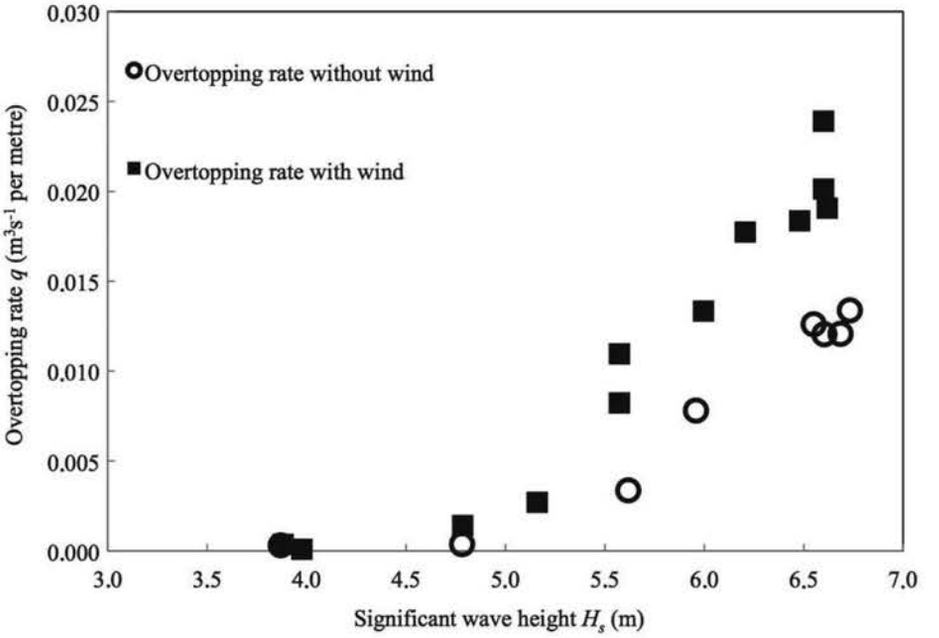

Figure 13 Comparison of the measured overtopping rates with and without wind at $T_p = 9$ s

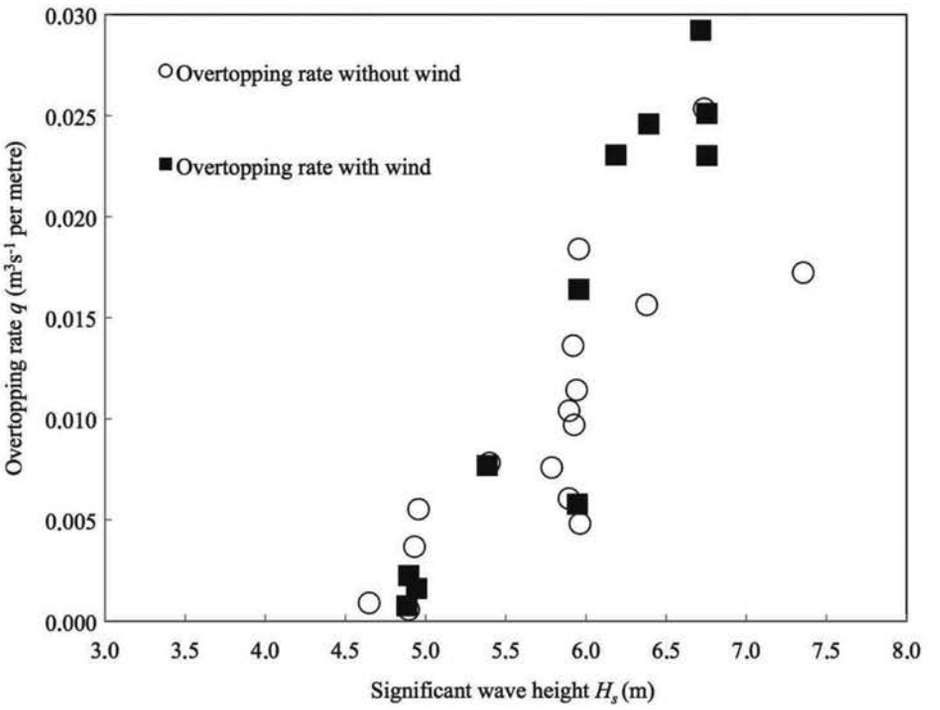

Figure 14 Comparison of the measured overtopping rates with and without wind at $T_p = 11$ s

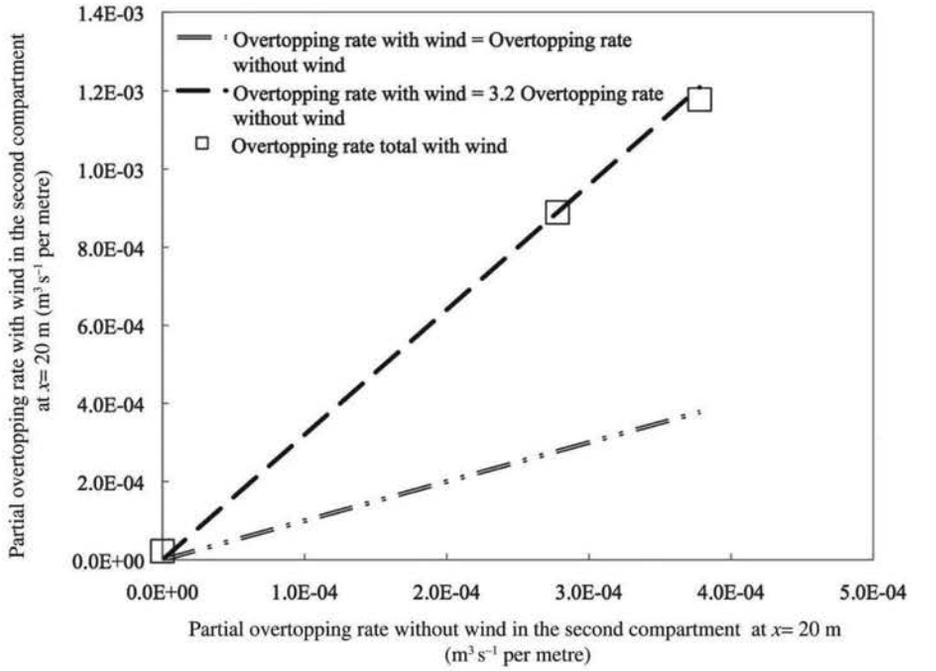

Figure 15 Partial overtopping rate with and without wind for the second compartment (distance from the crown wall is $x = 20$ m), $T_p = 9$ s

As to the pattern of the spatial distribution of the overtopping, the partial rates measured in the individual compartments do not show any significant differences in the tests with and without wind except for the compartment located 20 m from the crown wall. In this compartment, the overtopping rate measured with wind was three to four times that measured without wind (Fig. 15).

This observation agrees well with de Waal, Tönjes, & van der Meer (1996), who found that the overtopping rate measured with wind is approximately 3.2 times greater than the

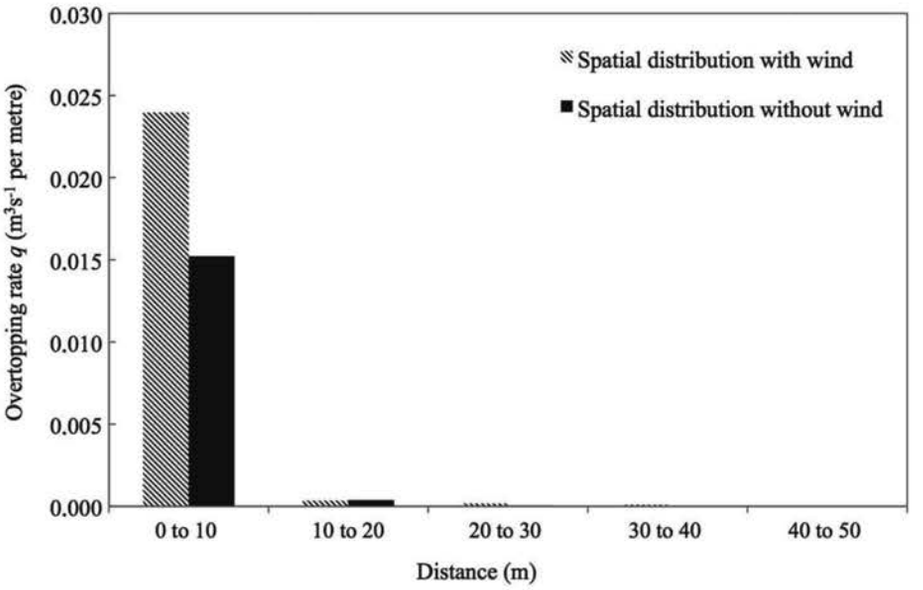

Figure 16 Spatial distribution of the overtopping rate with and without wind, $H_s = 6.5$ m and $T_p = 11$ s

rates recorded without wind. The spatial distribution of the overtopping rate for test situations with and without wind is shown in Fig. 16 where one can see that the wind significantly enhanced overtopping.

5 Conclusions

The results reported in this paper highlight a significant disparity between measured and predicted overtopping rates, showing very limited predictive power of the available relationships and approaches. All formulas considered in this paper have been obtained from laboratory tests and, therefore, are only valid for the geometrical (standard cross-section) and hydrodynamic (wave action, water level) conditions reproduced in these tests. However, the ranges of assumed applicability of the formulas do not fully match those of the presented tests. For example, when applying the Aminti & Franco (1988) formula, a good match is obtained between the predicted and measured rates, despite the fact that this equation was not tested for conditions of our experiments.

Taking the analysis of the validity of the equations' applicability into consideration, the best results were obtained when using the Berenguer & Baonza (2006) formula. When applying the NN-OVERTOPPING2 neural network of De Rouck et al. (2005), the predicted overtopping rates may deviate from the measured values by up to 100%. However, the comparison of this tool with the data is deemed incomplete (only four tests have been used for comparison) and therefore additional tests are required.

The results also show that wind modifies the way in which overtopping occurs and how waves interact with the structure, particularly in vertical breakwaters, supporting earlier studies of de Waal et al. (1996). In the tests performed with wind and waves, water drops have been seen to spread out more than in the case of windless tests. Although the total volumes of overtopping water with and without wind are not much different, the submergence is noticeably higher under the simultaneous action of wind and waves.

Funding

We appreciate the financial support provided by the Public State Ports Agency and the Port Authorities of Bilbao, Ferrol, Malaga and Alicante.

Notation

a	=	empirical coefficient (–)
A_c	=	armour crest freeboard of structures (m)
b	=	empirical coefficient (–)
B	=	width of structure crest (m)
F	=	width of parapet (m)
g	=	acceleration due to gravity (9.81 m s^{-2})
h_s	=	water depth at toe of structures (m)
h_*	=	discriminating parameter (–)
h_f	=	height of parapet (m)
H_s	=	significant wave height (m)
H_{m0}	=	estimate of significant wave height from spectral analysis (m)
$H_0{}'$	=	equivalent deep-water significant wave height (m)
N_0	=	number of waves (–)
t_0	=	observation time (s)
T_m	=	average wave period (s)
T_{0m}	=	average wave period at deep water (s)

T_{0p} = peak wave period at deep water (s)
T_p = spectral peak wave period (s)
q = overtopping rate per unit structure width (m^3 s^{-1} per metre)
$q_{estimated}$ = overtopping rate estimated when applying the empirical formulae and neural network (m^3 s^{-1} per metre)
$q_{measured}$ = mean overtopping rate measured in the tests (m^3 s^{-1} per metre)
Q = dimensionless overtopping rate (–)
R = dimensionless freeboard (–)
V_i = volume of overtopping wave per unit crest width (m^3 per metre)
α = angle between overall structure slope and horizontal (°)
γ = correction factor (–)
γ_b = correction factor for a berm (–)
γ_r = correction factor for the permeability and roughness (–)
γ_h = correction factor for deep (–)
γ_β = correction factor for oblique wave attack (–)
ε_{op} = Iribarren number or surf similarity parameter based on s_{op} (–)
L_0 = deep water wave length (m)
L_{0m} = mean wave length in deep water (m)
L_{0p} = peak wave length in deep water (m)
$R_{u2\%}$ = run-up level exceeded by 2% of incident waves (m)
s_{om} = wave steepness with L_{0m} (–)
s_{op} = wave steepness with L_{0p} (–)
$U_{wprototype}$ = wind speed in prototype (m s^{-1})

References

Ahrens, J. P., & Heimbaugh, M. S. (1988). Seawall overtopping model. *Proceedings of the International Conference on Coastal Engineering*, *21*, 795–806. Retrieved from https://icce-ojs-tamu.tdl.org/icce/index.php/icce/article/view/4266/3947

Allsop, N. W. H., Besley, P., & Madurini, L. (1995). *Overtopping performance of vertical and composite breakwaters, seawalls and low reflection alternatives*. Alderney: MCS Project Workshop.

Aminti, P., & Franco, L. (1988). Wave overtopping on rubble mound breakwaters, *Proceedings of the International Conference on Coastal Engineering*, 21, 770–781. Retrieved from https://icce-ojs-tamu.tdl.org/icce/index.php/icce/article/view/4264/3945

Berenguer, J. M., & Baonza, A. (2006). Diseño del espaldón de los diques rompeolas [Design of crown wall]. *Congreso Nacional de la Asociación Técnica de Puertos y Costas*, *2*, 35–46.

Bradbury, A. P., Allsop, N. W. H. & Stephens, R. V. (1988). *Hydraulic performance of breakwater crown walls* (Report SR 146). Wallingford: Hydraulic Research.

De Rouck, J., Boone, C., & Van de Walle, B. (2001). *The optimisation of crest level design of sloping coastal structures through prototype monitoring and modelling*. *OPTICREST* (Final report). Ghent: Ghent University.

De Rouck, J., Van de Walle, B., & Geeraerts, J. (2005). *Final report, full scientific and technical report. CLASH: Crest level assessment of coastal structures by full scale monitoring, neural network prediction and hazard analysis on permissible wave overtopping* (Report No. D46). Ghent: Ghent University.

de Waal, J. P., & van der Meer, J. W. (1992). Wave runup and overtopping on coastal structures. *Proceedings of the International Conference on Coastal Engineering*, *23*, 1758–1771. Retrieved from https://icce-ojs-tamu.tdl.org/icce/index.php/icce/article/view/4812/4493

de Waal, J. P., Tönjes, P., & van der Meer, J. W. (1996). Wave overtopping of vertical structures including wind effect. *Proceedings of the International Conference on Coastal Engineering*, *25*, 2216–2229. Retrieved from https://icce-ojs-tamu.tdl.org/icce/index.php/icce/article/view/5376

Franco, L., de Gerloni, M., & van der Meer, J. W. (1994). Wave overtopping on vertical and composite breakwaters. *Proceedings of the International Conference on Coastal Engineering*, *24*, 1030–1045. Retrieved from https://icce-ojs-tamu.tdl.org/icce/index.php/icce/article/viewFile/5015/4695

Goda, Y. (1985). *Random seas and design of maritime structures*. Singapore: World Scientific.

Grüne, J. (1982). Wave runup caused by natural storm surge waves. *Proceedings of the International Conference on Coastal Engineering*, *18*, 785–803. Retrieved from https://icce-ojs-}{tamu.tdl.org/icce/index.php/icce/article/view/3661/3344

Kingston, K., & Murphy J. (1996). *Thematic report B. Wave run-up/run-down* (Report No. MAS02/1-893/PTH). Cork: University College Cork.

Owen, M. W. (1980*). Design of seawalls allowing for wave overtopping* (Report No. Ex 924). Retrieved from http://eprints.hrwallingford.co.uk/551/1/EX924.pdf

Owen, M. W. (1982). The hydraulic design of sea-wall profiles. *Proceedings of the International Conference on Shoreline Protection*, *1*, 185–195.

Pedersen, J. (1992). Wave forces on crown walls. *Proceedings of the International Conference on Coastal Engineering*, *23*, 1489–1502. Retrieved from https://icce-ojs-tamu.tdl.org/icce/index.php/icce/article/view/4792/4473

Pedersen, J. (1996). *Wave forces and overtopping on breakwaters crown walls: an experimental study.* (Master's thesis). Aalborg University, Denmark.

Pullen, T., Allsop, N. W. H., Bruce, T., Kortenhaus, A., Schüttrumpf, H., & van der Meer, J. W. (2007). *EurOtop: Wave overtopping of sea defences and related structures:*

Assessment manual. Retrieved from http://www.overtopping-manual.com/eurotop.pdf

van der Meer, J. W. & Janssen, P. F. M. (1995). Wave runup and wave overtopping at dikes and revetments (Report No. 485). Retrieved from http://www.vandermeerconsulting.nl/downloads/functional_a/1994_vandermeer_janssen.pdf

Ward, D., Zhang, J., Wibner, C., & Cinotto, C. (1996). Wind effects on runup and overtopping of coastal structures. *Proceedings of the International Conference on Coastal Engineering*, *25*, 2206–2215. Retrieved from https://journals.tdl.org/icce/index.php/icce/article/view/5375/5052